

Technology for porous ammonium nitrate production: modeling of drying machines' operating modes

Nadiia ARTYUKHOVA¹, Jan KRMELA^{2*}, Artem ARTYUKHOV¹, Vladimíra KRMELOVÁ³,
Mária GAVENDOVÁ³, and Alžbeta BAKOŠOVÁ²

¹Sumy State University, Oleg Balatskyi Academic and Research Institute of Finance, Economics and Management, Department of Marketing, Rymkogo-Korsakova st. 2, 40007, Sumy, Ukraine

²Alexander Dubček University of Trenčín, Faculty of Industrial Technologies in Púchov, Department of Numerical Methods and Computational Modeling, Ivana Krasku 491/30, 020 01 Púchov, Slovakia

³Alexander Dubček University of Trenčín, Faculty of Industrial Technologies in Púchov, Department of Material Technologies and Environment, Ivana Krasku 491/30, 020 01 Púchov, Slovakia

Abstract. The article deals with the technological principles regarding the final drying process of porous ammonium nitrate (PAN) granules in multistage gravitational shelf dryers. The data on the dryers' optimal technological operating modes are obtained. PAN samples are studied; the regularity of porous structure change in the granule, depending on the dryers' hydrodynamic and thermodynamic conditions, is also established. Experimental data obtained during the research will be used to create a methodology for the engineering calculation of gravitational shelf dryers. Moreover, the data on the optimal operating conditions of drying machines at the final drying stage will be used to improve the technology to form porous granules from agricultural ammonium nitrate.

Key words: porous ammonium nitrate drying machine; operating modes; software.

1. INTRODUCTION

Porous ammonium nitrate (PAN) is a necessary component of the industrial explosive ANFO [1]. It consists of PAN and liquid fuel, mainly mineral oils, and acts as an effective substitute for industrial explosives (dynamites, TNT and mixtures containing TNT). PAN can successfully absorb and retain fuel oil due to the network of pores with different configurations and sizes in the granule porous structure. It is possible to obtain this system of pores in different ways [2–23]. Following the analysis of works [24–26] and the authors' research [27–29], this article proposes a method consisting of two stages to obtain PAN. During the first stage, agricultural ammonium nitrate is moistened with water or a particular solution in the vortex granulator's workspace or outside of it. During the second stage, the moistened granules are dried in a flow of hot heat transfer agent. The second stage requires special attention in ensuring the required drying time while maintaining the granule's strength properties. The study [30] proposes to carry out the drying process in two stages using two types of devices with directed motion of the fluidized bed to obtain the strength of the granule core.

The final drying process is carried out in a multistage dryer. There are different hydrodynamic conditions [31] for the motion of granules at its every stage [32, 33].

The aim of the article is to study and describe the main operating modes of a gravitational shelf dryer and to assess the effect made by the operating mode of the device on the PAN granules structure. A scheme of using a vortex granulator as the primary device and a shelf dryer at the final drying stage is a fundamental technological scheme to obtain PAN (see Fig. 1) [34, 35]. The applicability of such a scheme is justified in the works [30, 36].

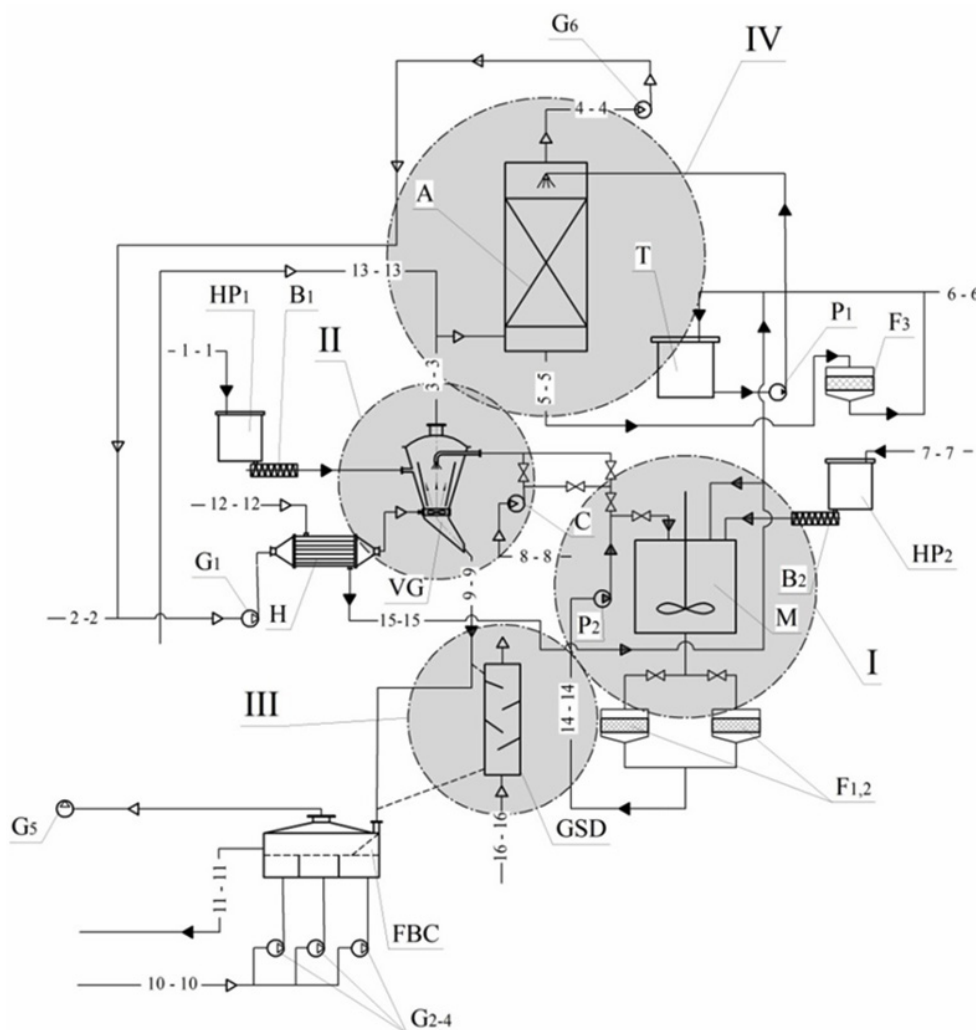
2. PHYSICAL MODEL OF FLOW MOTION HYDRODYNAMICS AND THE DRYING PROCESS OF DISPERSED MATERIALS IN A SHELF DRYER

The tilted perforated shelves in the shelf dryer's workspace decrease its free cross-sectional area. This construction decision causes a local increase in the velocity and degree of the drying agent's flow turbulence and changes the nature of the velocity's distribution around the shelf [30].

At certain flow velocities of the drying agent (much less than in the case of the first critical velocity), the material, which is being constantly fed into the dryer, moves along the surface of the tilted perforated shelf in the form of a "fast" layer that slips along it. This motion of particles occurs when they still have sufficient inertia force at the exit of the feeding device (dispenser). When the drying agent's flow rate increases, the porosity of the "fast" layer approaches the maximum and its structure becomes a weighted layer with the ablation of fine fractions. After passing along the tilted perforated shelf, the material particles begin to

*e-mail: jan.krmela@tnuni.sk

Manuscript submitted 2020-10-13, revised 2021-05-14, initially accepted for publication 2021-05-15, published in August 2021

**Legend:****Elements of the unit:**

- VG – vortex granulator;
- H – heater;
- GSD – gravitational shelf dryer;
- FBC – fluidized bed cooler;
- A – absorber;
- F – filter;
- M – mixer;
- B – batcher;
- HP – hopper;
- G – gas blower;
- P – pump;
- T – tank;
- C – compressor.

The main flows:

- 1-1 – seeding agent;
- 2-2 – manufacturing air;
- 3-3 – polluted air;
- 4-4 – purified air;
- 5-5 – polluted water;
- 6-6 – water;
- 7-7 – substandard granules;
- 8-8 – air for the spraying of liquid materials (solution, melt);
- 9-9 – product;
- 10-10 – air for cooling granules;
- 11-11 – granules for packaging;
- 12-12 – steam;
- 13-13 – dusty gas;
- 14-14 – liquid materials (solution, melt);
- 15-15 – water condensate;
- 16-16 – drying agent.

Fig. 1. A unit producing PAN granules by means of using a vortex granulator and a gravitational shelf dryer [28]

slow as they reach the dryer's walls in the outloading space, gathered near the surface of the walls. The dispersed phase layer is blown by the drying agent's ascending flow; while the layer mass gradually increases due to the new particles of the dispersed phase. This process lasts until the disbalance between particle gravity force and the aerodynamic force of its interaction with the ascending flow is settled. When the "critical" mass of the dispersed phase is accumulated and the forces balance is disturbed, a share of the material is removed from the stage through the outloading space. Given the above-described nature of the material motion on the tilted shelf surface and in the outloading space, the aerodynamic forces of the ascending flow restrain the solid particles motion only to some extent. Their bulk moves in a thin layer influenced by gravitational force. This nature of motion is called "gravitational falling layer".

Thus, the "gravitational falling layer" mode is characterized by the minimum required contact time of the particles with the drying agent, caused by a sufficiently high velocity of the particles. Therefore, the drying process in this mode on the shelf surface is limited not by hydrodynamic conditions, but by the length of the shelf, on the surface of which the particles move

quickly enough with minimum residence time. The latter will increase slightly in the particle accumulation zone in the form of a layer on the device's wall. As a result, we obtain more active phase contact and, accordingly, more intensive moisture removal from the particles by the drying agent in this zone. For the "gravitational falling layer" mode, implemented on the upper shelf (in the direction of the material flow), the material particles are heated. Thus, the process on the top shelf, implemented within a short period, corresponds to heating the material with slight removal of surface moisture with increasing drying velocity. The beginning of the moisture motion from the inner layer to the particles' surface is also observed. Usually, the heating period is insignificant in comparison with other drying periods. If particles' residence time on one shelf is less than the kinetically required heating time, there should be several shelves operating in the "gravitational falling layer" mode in the dryer's upper part.

The drying agent's velocity rise intensifies its aerodynamic effect on the material layer, creating conditions for the weighted layer mode on the surface of the perforated shelf and near the wall of the device in the outloading gap zone. When the drying agent in the form of a jet leaves the outloading gap, a high-pres-

sure area is formed. Some kinetic energy of the drying agent's moving flow is spent on compensating for the friction force that leads to its inhibition. The dispersed phase, which moves in this zone and is characterized by a small kinetic energy reserve, comes to the weighted layer. The small phase, which during outloading from the tilted shelf surface has insufficient inertia force to compensate for kinetic energy of the air flow, repeats the drying agent's jet trajectory leaving the outloading space, picked up by it, and then moves into the separation zone to the outlet pipe of the drying agent from the device. The polydisperse system is divided into two fractions in the separation zone. Larger particles, the growing velocity of which is greater than the airflow velocity in the cross-section of the device, move down to the shelf surface. The airflow ablates smaller particles from the device.

In the weighted layer mode, moisture removal efficiency from the material is significantly increased due to the intensification of phase contact because the particles actively interact with the airflow both on the perforated shelf surface and in the outloading area. Since reducing the size of the gap between the end of the shelf and the wall of the device increases the velocity of the airflow entering the weighted layer of material through the outloading space, this is the main factor in intensifying phase contact and, consequently, mass transfer process. The increase in the particles' residence time due to their mass circulation in the zone above the outloading space facilitates the moisture transfer growth from the material particles in the weighted layer mode. Therefore, considering the hydrodynamic features of the weighted layer, in this mode, the wet material is dried quite effectively in periods of constant (first period) and falling (second period) velocity.

Since the longest duration in time describes the drying kinetics in the falling velocity period, the number of shelves in the lower part of the dryer is selected to complete moisture removal according to the technological requirements.

The motion of the dispersed phase on each of the shelf cascades is qualitatively the same. Some zones of its motion along the dryer's cross-section, depending on the height of the shelf, can be of different lengths. As it moves along the dryer's height, the drying agent slightly reduces its velocity due to the drag force along the length and local resistance. The drying agent's velocity is not significantly changed but still leads to different dispersed phase motion modes. One can observe faster motion of particles along the shelf length on the upper shelf of the cascade, with the accumulation of less material on the walls. When the particles come close to the place of the drying agent's injection, their velocity on the shelf begins to decrease. This situation is hardly noticed, but experimental studies confirm it.

Changes in the constructive parameters of the dryer's shelf contacts provide the necessary hydrodynamic conditions for the material motion on each shelf of the cascade. When constructing a gravitational shelf dryer, it is required to ensure uniform contact of the drying agent with the dispersed material on each dryer shelf. Achieving such uniformity enables regulating the particles' residence time on the shelves, allowing for their physicochemical properties. Any uneven contact of the drying agent with the dispersed material can lead to underheating (with

insufficient drying) or overheating with undesirable destruction of particles and reducing its qualities.

Thus, the minimum required contact time of the dispersed material (with physicochemical properties, granulation composition and drying agent's parameters) is provided by means of varying the length, installation angle or perforation degree of the upper shelf. The small fraction is removed from this shelf, i.e. it acts as a separator. The residence time of the dispersed material grows on the central inclined contact shelf, changing its constructive parameters, and, accordingly, its contact with the drying agent increases. It promotes more intensive removal of moisture. The connection between the dispersed material and the drying agent on the lower inclined contact shelf provides long residence time for the particles on the shelf to remove moisture from the material.

3. OPERATING MODES OF THE GRAVITATIONAL SHELF DRYER

The experimental unit of the multistage shelf dryer is shown in Fig. 2.

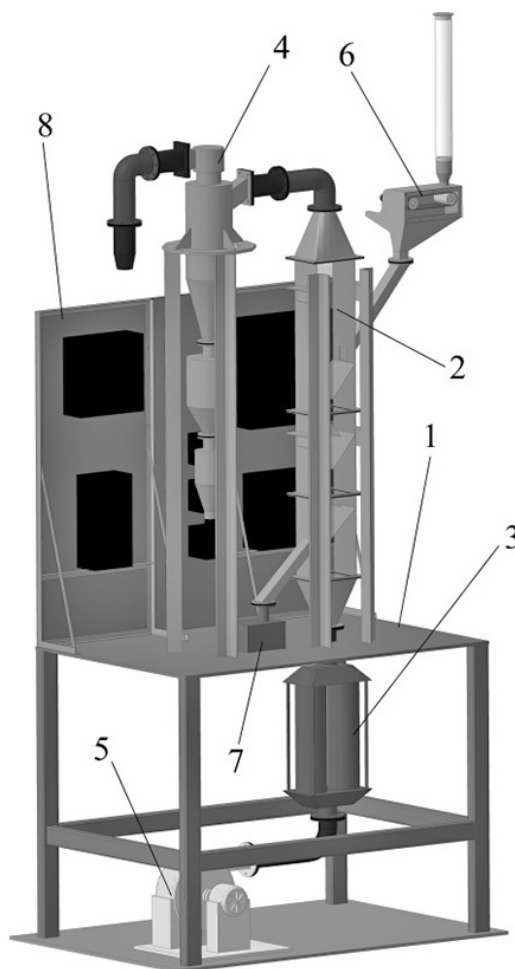


Fig. 2. Model of the experimental unit (final drying stage): 1 – supporting structure; 2 – shelf dryer; 3 – air heater; 4 – cyclone; 5 – blower; 6 – hopper of AN granules; 7 – hopper of PAN granules after final drying; 8 – process automation switchboard

During experimental studies of dispersed material motion in a shelf dryer, it becomes possible to identify the effect that the particle package motions have on each other (zones of packages collision, vortex formation, dispersed material motion with greater or lesser intensity, etc.). Model material: 1) investigation of dryer's hydrodynamics – 75% of polypropylene (diameter of granule is $d = (3.0-3.5)$ mm, granule's moisture content is $x = 1.7\%$) and 25% of ammonium nitrate ($d = (2.0-2.5)$ mm, $x = 0.2\%$); 2) investigation of ammonium nitrate porous structure morphology – ammonium nitrate ($d = (2.0-2.5)$ mm, $x = 0.2\%$). Water solution of AN was used for moistening AN granules in a vortex granulator.

The main modes of the dispersed material motion, defined by the experimental studies, include:

1. Gravitational falling layer mode (Fig. 3), investigated at the drying agent's flow rate of $24.6 \text{ m}^3/\text{h}$ and dispersed material of 12 kg/h . The dispersed material moves along the surface of the shelf due to the inertia force, caused by the transmission of momentum when loading from the pipe or when moving from the previous shelf, and force of rolling on the tilted surface. The drying agent's ascending flow force does not significantly affect the dispersed material motion mode. In this mode, the gas flow velocity is less than the first critical gas flow rate, which corresponds to the weighing mode.
2. First transitional mode (Fig. 4): drying agent's flow rate of $30 \text{ m}^3/\text{h}$, dispersed material flow rate of 12 kg/h . The ascending flow force of the drying agent in this mode leads to

a gradual change in its motion from pulse to the pulse-forward trajectory in the direction of the outloading gap. The dispersed material begins to transform into a weighted state, the inertia force value is compensated for by the drying agent's ascending flow force, and the gradual direction of motion is caused only by rolling force on the tilted surface. In this mode, the gas flow rate approaches the value of the first critical gas flow rate.

3. Weighted layer mode (Fig. 5): drying agent's flow rate of $(33-45) \text{ m}^3/\text{h}$, dispersed material flow rate of $(12-15) \text{ kg/h}$. The ascending flow force of the heat transfer agent in this mode leads to creating a stable weighted layer by compensating for the inertia and rolling force on the tilted surface. The gas flow rate reaches the first critical velocity. It grows subsequently and is in the operating velocity range.

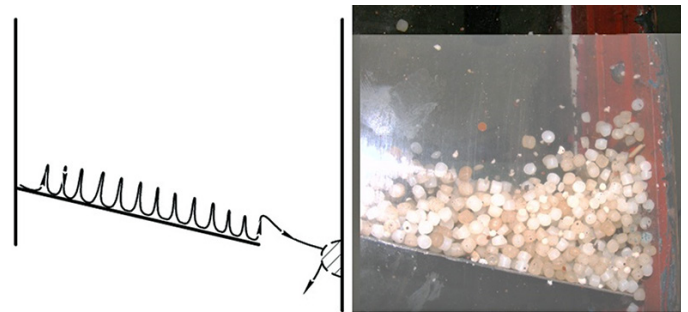


Fig. 5. Dryer's operation in the weighted layer mode of the dispersed material

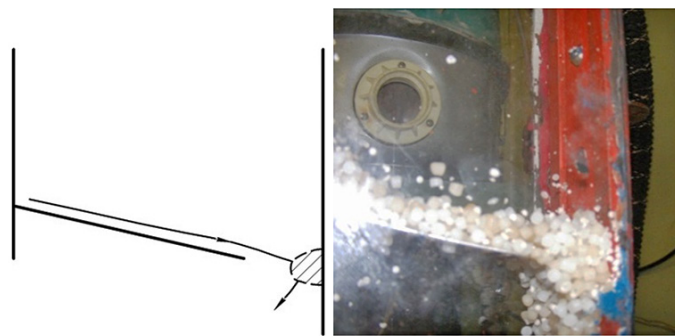


Fig. 3. Dryer's operation in the gravitational falling layer mode of the dispersed material

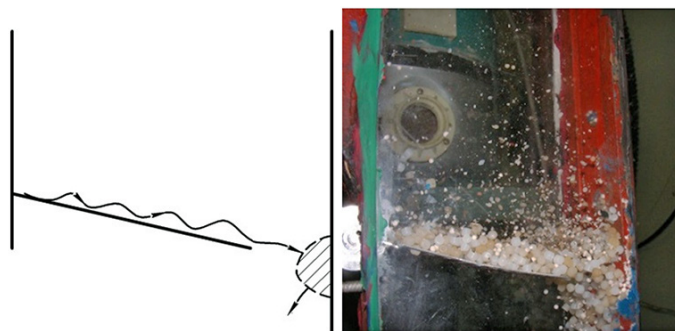


Fig. 4. First transitional mode of the dryer's operation

There are several zones on the dryer's contact shelf in this mode and in the outloading gap (Fig. 6). In the weighted layer 1



Fig. 6. Distinctive zones of dispersed material motion in the gravitational shelf device: 1 – weighted layer creation zone on the shelf; 2 – zone of lowering the weighted layer intensity; 3 – vortex creation zone; 4 – zone of increased velocity of the dispersed material motion over the outloading gap; 5 – separation zone of finely dispersed material; 6 – outloading zone of the dispersed material from the shelf

zone, the dispersed material moves due to its pulse-forward transfer to the outloading gap.

In the zone of lowering the weighted layer intensity 2 by decreasing the drying agent's velocity, caused by reduction of the pressure drop along the shelf, the dispersed material loses some vertical motion along the axis of the device.

The dispersed material moving to the end of the shelf passes through the vortex creation zone 3, formed by bending the shelf by the drying agent, and through the increased velocity zone over the outloading gap 4, and is then output from the shelf through zone 6. Under the drying conditions, the polydisperse material, i.e. the small fraction with the size defined by the calculations, is separated in zone 5.

4. Second transitional mode (Fig. 7): drying agent's flow rate of (36–47.3) m³/h, dispersed material flow rate of (12–13.5) kg/h. This mode is characterized by a predominant effect created by the ascending force on the dispersed material by increasing the vertical component of its motion. In this case, some dispersed material is ablated from the shelf surface before entering the outloading gap. Gas velocity for this mode varies between the calculated values of the first critical velocity and the ablation rate.



Fig. 7. Second transitional mode of the dryer's operation

5. Dispersed material ablation mode (Fig. 8): the drying agent's flow rate of 48 m³/h, dispersed material flow rate of 12 kg/h. It is characterized by an increase in the vertical component and the dispersed material ablation of the commodity fraction from the contact shelf without moving to the dryer's

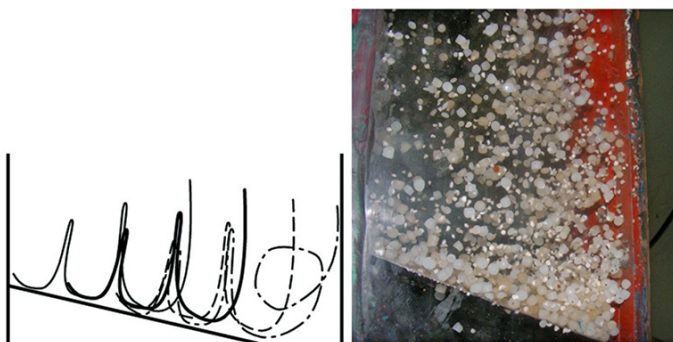


Fig. 8. Dryer's operation in the dispersed material ablation mode

next stage. The drying agent's ascending motion force significantly exceeds the sum of the inertia and rolling forces on the tilted surface, causing the forward motion of the dispersed material along the shelf. Gas velocity in the observed mode reaches the ablation rate of particles of this size from the device.

The data analysis from the studies on the shelf device's operating modes narrows its operating modes to the first three modes. In the fluidized bed mode of the dispersed material, small particles (due to the difference in critical velocities) leave the workspace with a high probability. Figure 9 shows diagrams of the gas flow relative velocities in the above-the-shelf space and the outloading gap for the three modes. Peak velocity in the outloading gap is the maximum relative velocity. According to this peak, it is possible to compare the value of the second critical velocity of the gas flow with the operating velocity and to conclude about the possible ablation of dispersed particles from the shelf.

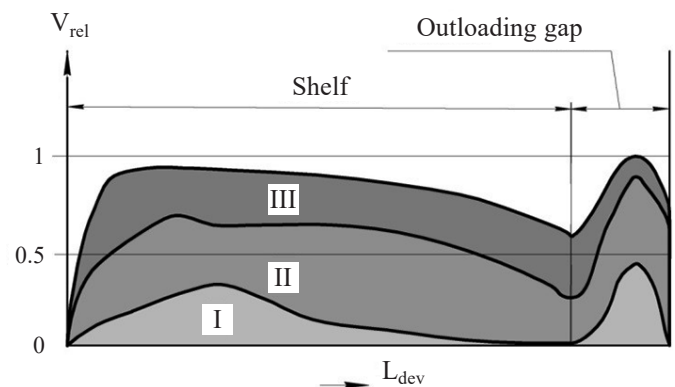


Fig. 9. Relative velocity of the gas flow over the dryer's shelf and in the outloading gap; I – gravitational falling layer mode; II – first transitional mode; III – fluidized bed mode

One should note that it is essential to identify (except for the gas flow rate) the residence time of the dispersed material on the shelf of the device in each dryer's operating mode. Using the [37] method, a graph of the relative residence time changing of the dispersed material in the device is obtained in this article (Fig. 10). In each mode, the nature of the change in residence time has its own increase intensity. On the horizontal axis in Fig. 10, the difference between the second critical velocity of the gas flow and its operating velocity is shown. On the vertical axis, the unit of relative time is taken to be the value that corresponds to the transition moment from the fluidized bed mode in the first transitional mode.

Analysis of Fig. 10 shows that it is possible to provide a longer residence time of the dispersed phase in the device in the transitional mode and at the beginning of the ablation mode. However, according to further studies on the crystal structure of the PAN granules, the excessive residence time in the workspace of the device (excessive contact with hot heat transfer agent) reduces the granule strength.

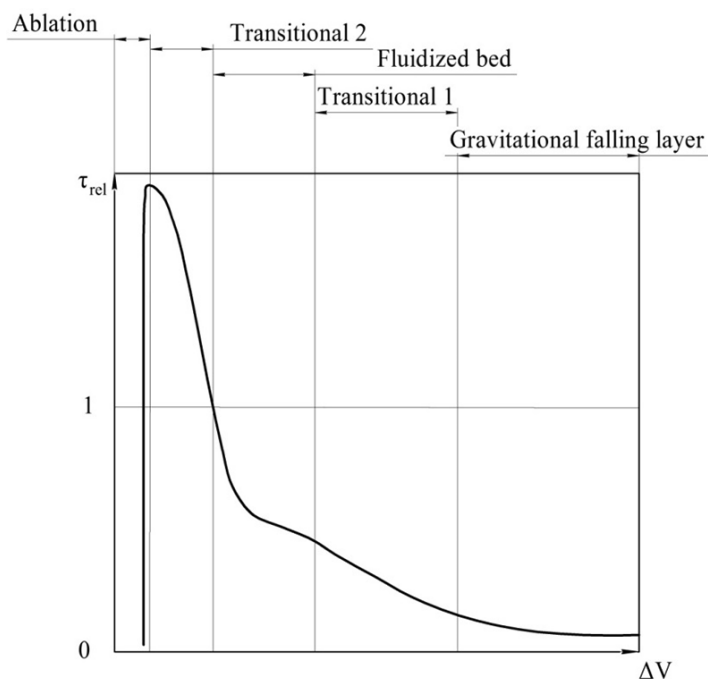


Fig. 10. Relative residence time of particles in the dryer at different modes

4. DEVICES, EQUIPMENT AND METHODS OF RESEARCH

Devices and equipment:

- used to determine the hydrodynamic features of the flow motion – TES 1340 Hot-Wire Anemometer;
- used for measurement of water content in granules – Fischer volumetric titrator HI903;
- used for measurement of granules' strength – extensometer, a device for measuring the strength;
- used for measurement of oil retention – small-sized corner centrifuge and centrifuged tube with two divisions (the first division has a perforated bottom; the second one has a plate bottom).

The hydrodynamic properties of the flow motion are measured at various points of the dryer, determined by a micro coordinator. The value is defined as the average of five measurements at each point.

The arithmetic mean of the results of water content in granules for two parallel determinations is taken to analyze the volumetric Fischer titration result, the absolute discrepancy between which does not exceed the repeatability limit of 0.02%, with a confidence level 0.95.

Granules with similar dimensions and shapes are taken to determine the strength of the granules. The force required to break each of the granules is determined. Strength is determined as the average of twenty measurements of force that destroys the granule.

Procedure of oil retention definition

The second division of the centrifuged tube is weighted. Six grams of ammonium nitrate and two grams of diesel fuel are

weighted, then placed in the glass, and mixed for five minutes using thin metal wire. The received mixture is left for 10 minutes and the complete mixture is off-loaded into the first division of the centrifuged tube. The full centrifuged tube is placed in the centrifuge and centrifuged for 10 minutes at 1500 rpm (rotations per minute). Once the process is finished, the second division of the centrifuged tube is weighted and then diesel fuel weight is defined.

Oil retention is defined as a proportion of the mass of oil absorbed by PAN to the PAN mass.

5. PAN GRANULE POROUS STRUCTURE

The crystal structure of the PAN granules at different stages of its production is studied to confirm the selected operating modes of the shelf dryer. Figures 11–16 show the scanning electron microscopy (scanning electronic microscope REM-100U) images of the granules porous layer. The main characteristics of the microscopic image are visible in the bottom part of images.

The figures show that the nature, structure and number of pores in the PAN depend on the heat treatment time and the contact mode between the drying agent and the granule.

After the final drying stage, the number of twisted pores on the PAN increased and it acquired a more uniform porous structure. This enables to intensify the process of fuel penetration into the granule. The bulk density of the granules does not change significantly.

Table 1 presents the results of the research.

Table 1
Properties of PAN granules

Mode	Description of structure of AN granule	Strength, kg/granule	Oil retention, %
AN granule (before humidification and drying)	a small number of shallow straight pores	0.50	5.30
AN granule after vortex granulator	many shallow straight pores, and twisted pores	0.45	8.10
PAN granule after shelf drying			
Gravitational falling layer	many shallow straight and twisted pores	0.43	8.40
First transitional mode	many shallow straight pores, formation of a network of straight and twisted pores	0.42	8.50
Fluidized bed	developed network of straight and twisted pores	0.40	8.80
Second transitional mode	developed network of straight and twisted pores, cracks	0.38	8.40

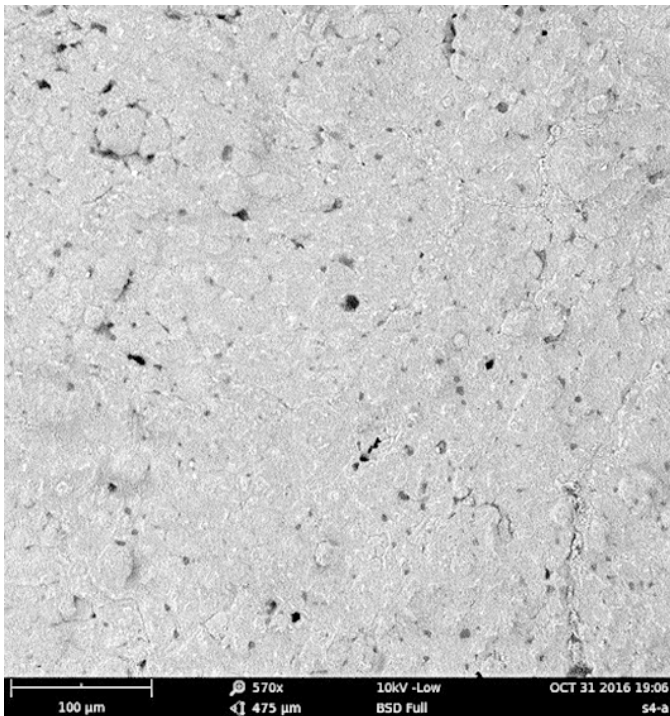


Fig. 11. Crystal structure of agricultural AN

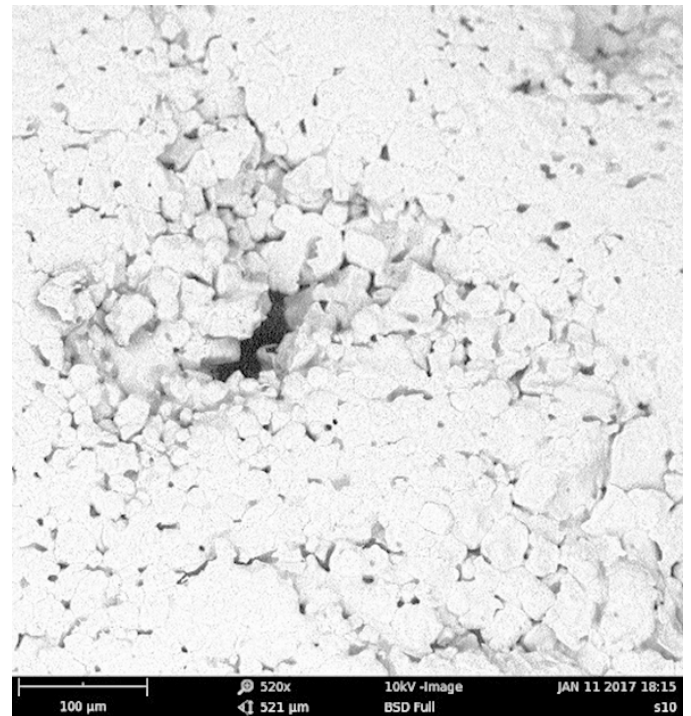


Fig. 12. Crystal structure of AN granule after humidification and heat treatment in a vortex granulator

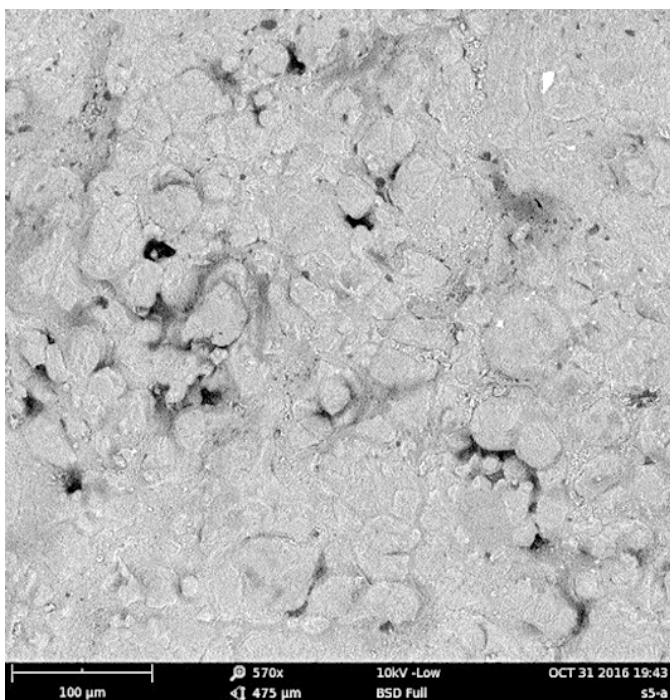


Fig. 13. Crystal structure of AN granule after final drying in the shelf device in the gravitational falling layer mode

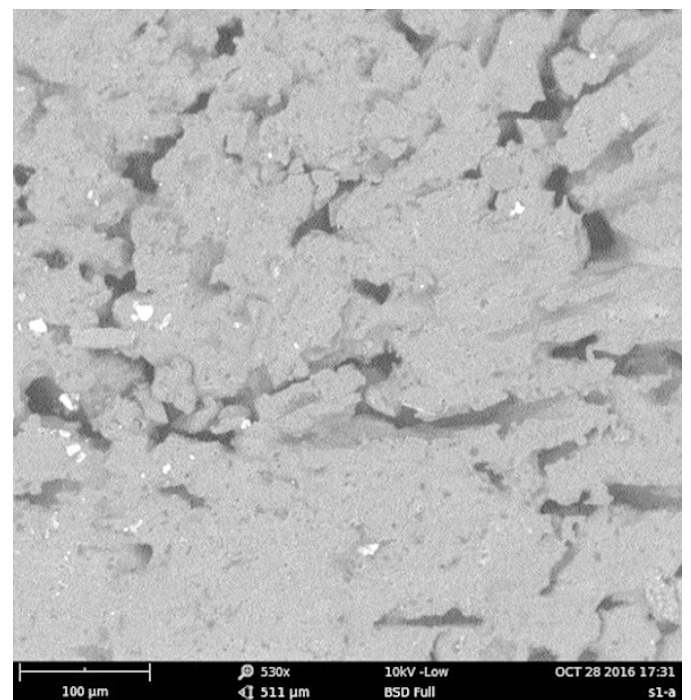


Fig. 14. Crystal structure of AN granule after final drying in the shelf device in the first transitional mode

The study results show that it is beneficial to intensify the operation of a gravitational shelf dryer. The dryer's optimal operating mode is the fluidized bed. Figure 10 shows that after this mode, the residence time of the granules in the device increases. An

increase in the drying time leads to the granules' overheating and temperature stresses in the core. As a result, the granules' strength goes down (pores appear in the granule core). And despite the increase in the gaps in the granule, oil retention goes down.

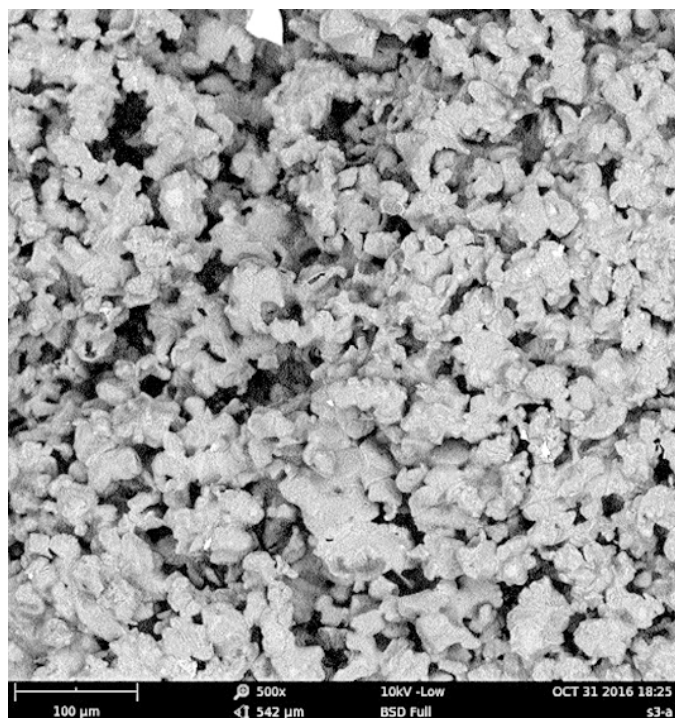


Fig. 15. Crystal structure of AN granule after final drying in the shelf device in the fluidized bed mode

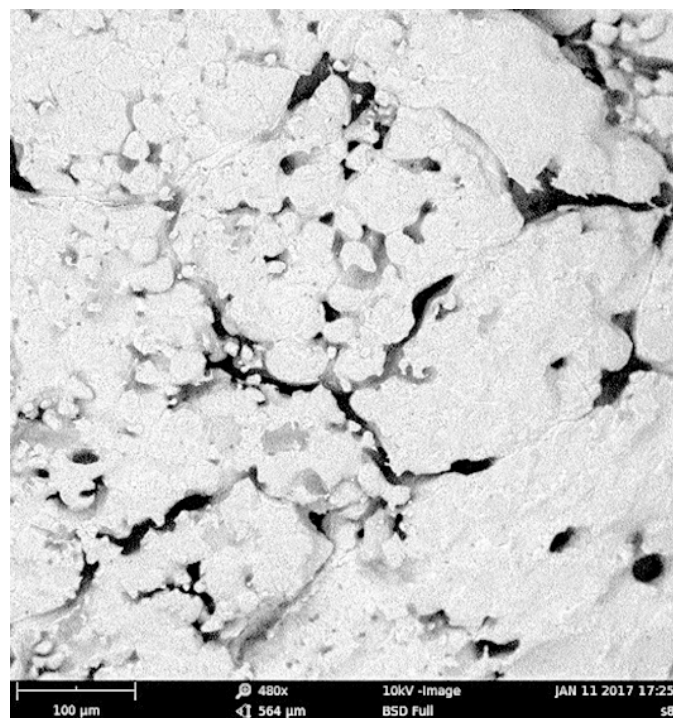


Fig. 16. Crystal structure of PAN granule after final drying in the shelf device in the second transitional mode

6. CONCLUSIONS

The results of investigation of multistage shelf devices' operating modes and PAN granules' crystal structure enable establishing the optimal range of dryer's operation at the final drying stage. The perforated shelf contact construction for each stage of the dryer is chosen by calculating the required residence time of the granule at the drying stage [37]. The main condition for selection: residence time of the granules in the vortex granulator and the shelf dryer should not be less than the estimated drying time. Based on this condition, there is an algorithm for optimizing the drying unit's calculation: selection of the number of steps, the length of the shelf, its perforation degree, the tilt angle to the horizon, etc. It is also planned to use the neural network [38, 39] to optimize the drying process for further research.

ACKNOWLEDGEMENTS

The authors would like to thank researchers at the Chemical Engineering Department, Sumy State University, and at the Department of Numerical Methods and Computational Modeling, Alexander Dubček University of Trenčín, for their valuable comments during article preparation.

This research work had been supported by the Cultural and Educational Grant Agency of the Slovak Republic (KEGA), project No. KEGA 002TnUAD-4/2019, "The influence of temperature and other parameters on the tensile properties of polymer composites and polymers under the uniaxial and biaxial cyclic loading" and Ministry of Science and Education of Ukraine, under the project No. 0120U100476, "Technological bases of multistage convective drying in small-sized devices with utilization and heat recovery units" and the project of advancement

and support of R&D for the "Centre for diagnostics and quality testing of materials" in the domains of the RIS3 SK specialization, ITMS2014: 313011W442.

REFERENCES

- [1] T.J. Janssen, *Explosive materials: classification, composition and properties*, Nova Science Publishers, Inc., New York, 2011.
- [2] Patent No. 5540793 US: Porous prilled ammonium nitrate, 1996.
- [3] Patent No. 2118074, CA: Porous prilled ammonium nitrate, 2002.
- [4] Patent No. 2093727, CA: Hardened porous ammonium nitrate, 2004.
- [5] Patent No. 2004-256365, JP: Method of manufacturing porous granular ammonium nitrate, 2004.
- [6] Patent No. 2005-350276, JP: Method for producing porous granular ammonium nitrate, 2005.
- [7] Patent No. 2221717, CA: Procedure and installation for the manufacture of porous ammonium nitrate, 2005.
- [8] Patent No. 102093146, CN: Microporous granular ammonium nitrate and preparation methods thereof, 2011.
- [9] Patent No. 102173968, CN: Production method of porous granular ammonium nitrate, 2011.
- [10] Patent No. 2452719, RU: Device for production of porous granulated ammonium nitrate and method for production of porous granulated ammonium nitrate, 2012.
- [11] Patent No. 391973, PL: Method for producing granulated porous ammonium nitrate, 2012.
- [12] Patent No. 103896695, CN: Microporous pellet ammonium nitrate and preparation method thereof, 2014.
- [13] Patent No. 204384319, CN: Device for producing porous ammonium nitrate and industrial ammonium nitrate, 2015.
- [14] Patent No. 204237724, CN: Recycling device for caked ammonium nitrate during production of porous ammonium nitrate, 2015.

- [15] Patent No. 104311372, CN: Porous ammonium nitrate production caking ammonium nitrate recycling apparatus and method of use, 2016.
- [16] Patent No. 106316727 CN: Porous and granular ANFO (ammonium nitrate fuel oil) and preparation method thereof, 2017.
- [17] Patent No. 2599170, RU: Method of producing porous granulated ammonium nitrate, 2016.
- [18] Patent No. 2600061, RU: Method of porous granulated ammonium nitrate producing and device for its implementation, 2016.
- [19] Patent No. 112294 UA: Device for granulation in the suspended layer, 2016.
- [20] Patent No. 112393 UA: Vortex granulator with utilization of waste gases, 2016.
- [21] Patent No. 112394 UA: Vortex granulator, 2016.
- [22] Patent No. 112622 UA: Vortex granulator, 2016.
- [23] Patent No. 113141 UA: Vortex granulator, 2017.
- [24] G. Martin and W. Barbour, *Industrial nitrogen compounds and explosives, Chemical Manufacture and Analysis*, Watchmaker Publishing, Seaside, 2003.
- [25] N. Kubota, *Propellants and explosives: thermochemical aspects of combustion*. 3rd ed., Wiley-VCH Verlag & Co., Weinheim, 2015.
- [26] D. Buczkowski and B. Zygmunt, "Detonation Properties of Mixtures of Ammonium Nitrate Based Fertilizers and Fuels", *Cent. Eur. J. Energetic Mater.*, vol. 8, no. 2, pp. 99–106, 2011.
- [27] A.E. Artyukhov and V.I. Sklabinskyi, "Experimental and industrial implementation of porous ammonium nitrate producing process in vortex granulators", *Naukovyi Visnyk Natsionalnoho Hirnychoho Universytetu*, vol. 6, pp. 42–48, 2013.
- [28] A.E. Artyukhov and N.A. Artyukhova, "Utilization of dust and ammonia from exhaust gases: new solutions for dryers with different types of fluidized bed", *J. Environ. Health Sci. Eng.*, vol. 16, no. 2, pp. 193–204, 2018.
- [29] A.E. Artyukhov and V.I. Sklabinskyi, "Investigation of the temperature field of coolant in the installations for obtaining 3D nanostructured porous surface layer on the granules of ammonium nitrate", *J. Nano- and Electron. Phys.*, vol. 9, no. 1, pp. 01015-1–01015-4, 2017.
- [30] N.A. Artyukhova, "Multistage finish drying of the N_4HNO_3 porous granules as a factor for nanoporous structure quality improvement", *J. Nano- and Electron. Phys.*, vol. 10, no. 3, pp. 03030-1–03030-5, 2018.
- [31] J. Hahm and A. Beskok, "Numerical simulation of multiple species detection using hydrodynamic/electrokinetic focusing", *Bull. Pol. Acad. Sci. Tech. Sci.*, vol. 53, no. 4, pp. 325–334, 2005.
- [32] A.E. Artyukhov, V.K. Obodiak, P.G. Boiko, and P.C. Rossi, Computer modeling of hydrodynamic and heat-mass transfer processes in the vortex type granulation devices, in *CEUR Workshop Proceedings*, vol. 1844, pp. 33–47, 2017.
- [33] A.E. Artyukhov, N.O. Artyukhova, and A.V. Ivaniia, "Creation of software for constructive calculation of devices with active hydrodynamics", in *Proceedings of the 14th International Conference on Advanced Trends in Radioelectronics, Telecommunications and Computer Engineering (TCSET 2018)*, 2018, pp. 139–142.
- [34] A.E. Artyukhov, N.A. Artyukhova, A.V. Ivaniia, and J. Gabrusenoks, "Multilayer modified NH_4NO_3 granules with 3D nanoporous structure: effect of the heat treatment regime on the structure of macro- and mezopores", in *Proc IEEE International Young Scientists Forum on Applied Physics and Engineering (YSF-2017)*, 2017, pp. 315–318.
- [35] A.E. Artyukhov and J. Gabrusenoks, "Phase composition and nanoporous structure of core and surface in the modified granules of NH_4NO_3 ", *Springer Proc. Phys.*, vol. 210, pp. 301–309, 2018.
- [36] N.O. Artyukhova and J. Krmela, "Nanoporous structure of the ammonium nitrate granules at the final drying: The effect of the dryer operation mode", *J. Nano- Electron. Phys.*, vol. 11, no. 4, pp. 04006-1–04006-4, 2019.
- [37] V.K. Obodiak, N.O. Artyukhova, and A.E. Artyukhov, "Calculation of the residence time of dispersed phase in sectioned devices: Theoretical basics and software implementation" *Lect. Notes Mech. Eng.*, pp. 813–820, 2020.
- [38] B. Paprocki, A. Pregowska, and J. Szczepanski, "Optimizing information processing in brain-inspired neural networks", *Bull. Pol. Acad. Sci. Tech. Sci.*, vol. 68, no. 2, pp. 225–233, 2020, doi: [10.24425/bpasts.2020.131844](https://doi.org/10.24425/bpasts.2020.131844).
- [39] W. Jefimowski A. Nikitenko Z. Drajek, and M. Wiczorek, "Stationary supercapacitor energy storage operation algorithm based on neural network learning system", *Bull. Pol. Acad. Sci. Tech. Sci.*, vol. 68, no. 4, pp. 733–738, 2020, doi: [10.24425/bpasts.2020.134176](https://doi.org/10.24425/bpasts.2020.134176).